Effect of soil variability on nonlinear site response predictions: Application to the Lotung site

Effect of soil variability on nonlinear site response predictions: application to the Lotung site

Yusuf Guzel[1], Mohamed Rouainia[1], Gaetano Elia[2]

[1] *School of Civil Engineering, Newcastle University, Newcastle upon Tyne, NE1 7RU, UK*
[2] *DICATECh, Technical University of Bari, 70126 Bari, Italy*

Abstract

The shear wave velocity profile and dynamic soil properties are the main factors controlling the results of ground response analyses for a given bedrock input motion. They are known to be spatially variable and adequate consideration of their variability may lead to a better prediction of the site response. Furthermore, the elastic and nonlinear dynamic properties of a soil deposit depend on the constitutive model adopted to describe the soil mechanical behaviour during the seismic oscillation. This paper aims to investigate the effect of a statistical variation in the initial stiffness profile, stiffness degradation and damping curves on ground response predictions by conducting Monte Carlo (MC) simulations. The Large Scale Seismic Test (LSST) site in Lotung, Taiwan, is back-analysed using a fully-coupled finite element procedure and applying at bedrock level one strong and one weak motion recorded at the site. A kinematic hardening soil model, capable of capturing the stiffness degradation and damping data measured from laboratory tests, is adopted in the analysis. The results of the statistical analysis indicate that the effect of variability in the elastic and nonlinear soil properties on the LSST site response predictions is very sensitive to the seismic intensity of the input motion. When the level of induced shear strain is higher, i.e. in the case of the stronger motion, the spatial variability of the stiffness degradation and damping curves has a pronounced effect on the predicted site response. In contrast, the prediction is particularly sensitive to the statistical variation in the initial stiffness profile when the weaker motion is considered. This is mainly due to the early stiffness degradation at very small strains shown by the laboratory data on LSST soils, which is described in the paper by assuming an appropriate elastic domain in the constitutive model calibration.

Keywords: Nonlinear site response analysis, Constitutive modelling, Soil properties, Monte Carlo simulations, Uncertainty

1. Introduction

Ground response analysis is a key tool in the seismic design of geotechnical structures, buildings and infrastructures. To predict local site effects, seismic input motions are propagated through the deposit approximating the dynamic characteristics of the soil by means of equivalent linear or nonlinear approaches. The results of the simulations are, then, interpreted mostly in terms of response spectra and amplification factors obtained at surface [1]. Nonlinear soil behaviour can be approximated by an equivalent linear characterisation of soil dynamic properties. The method, which represents the state-of-practice approach to quantify local site effects, makes use of the exact continuum solution of wave propagation in horizontally layered visco-elastic materials subjected to vertically propagating transient motions [2]. It models the nonlinear variation of soil shear modulus (G) and damping (D) using of linear analyses with iterative update of stiffness and damping parameters. For a given soil layer, G and D are assumed to be constant with time during the shaking. Therefore, an iterative procedure is needed to ensure that the properties used in the linear dynamic analyses are consistent with the level of strain induced in each layer by the input motion [1]. The analysis is performed within a total stress approach. Nonlinear time-domain schemes are also widely adopted in the literature for ground response analyses. Kaklamanos et al. [3] compared the results of linear, equivalent linear and nonlinear site response analyses of 191 ground motions recorded at six validation sites in the KiK-net array network (Japan). They have showed that all models tend to under-predict surface motions at short periods (< 0.2 s) and that there are relatively small differences in the accuracy between nonlinear and equivalent linear methods. Zalachoris and Rathje [4] also concluded that both nonlinear and equivalent linear analyses under-predict surface motions at short periods (< 0.4 s) and large strains by 55 to 65%. However, it should be noted that the nonlinear analyses in these studies were performed adopting a total stress approach and relatively simple soil constitutive models. In contrast, nonlinear effective stress approaches used in conjunction with advanced constitutive assumptions are capable of fully capturing soil nonlinearity, pore water pressure build-up and consolidation settlements induced by the earthquake, thus leading to more accurate results. In particular, the benefit of time-domain nonlinear schemes can be fully appreciated when the site is shaken by a strong seismic motion [e.g. 5].

The free-field seismic response prediction under a single bedrock motion is controlled by the elastic and nonlinear soil properties, i.e. the initial shear wave velocity (V_s) profile, the normalized shear modulus (G/G_0) reduction and damping ratio curves. The V_s profile of a soil deposit is commonly measured by means of in-situ tests, such as cross-hole, down-hole, seismic cone, MASW

(Multichannel Analysis of Surface Waves), SASW (Spectral Analysis of Surface Waves), suspension logging methods [e.g. 1]. The standard penetration test (SPT) and the cone penetration test (CPT), although originally developed for the measurement of soil properties mobilised at large strains, can be indirectly used to determine in-situ shear modulus profiles by using empirical correlations between penetration resistance (NSPT) or tip resistance (q_c) values and G_{max}. These estimates are affected by high uncertainties and should be used very cautiously for a preliminary assessment of G_{max}, given the scatter in the data on which they are based and the variability in the results obtained by different correlations. The shear modulus degradation and associated hysteretic damping can be determined over a range of shear strains through laboratory testing of undisturbed soil samples (e.g. resonant column/torsional shear, cyclic triaxial and cyclic simple shear tests). Nevertheless, it is most common to use published modulus reduction and damping curves [e.g. 6, 7, 8] rather than performing direct measurements of these soil dynamic properties in the laboratory.

Although site response analysis usually adopts the deterministic values of the elastic and nonlinear soil properties, their uncertainty and variability in space, even within a single soil layer, should be taken into account [e.g. 9]. In this respect, the effect of soil properties variability on site response predictions is nowadays of great interest for researchers in the geotechnical earthquake engineering field [e.g. 10, 11, 12, 13, 14, 15, 16, 17, 18, 19, 20, 21]. Most commonly, the variability of soil dynamic properties is accounted for just using the upper/lower bounds of the V_s profiles and modulus degradation and damping curves generated from statistical models. A more robust way of including the variability of the soil properties in site response analyses is through Monte Carlo (MC) simulations [e.g 22]. They employed a stochastic finite-fault model able to produce a seismic motion with a specific magnitude and distance from the fault. The model was also capable of accounting for soil property variability within an equivalent linear formulation. The results indicated that i) site effects variability is clearly a function of the distance (and, therefore, of the seismic intensity level); ii) path effects have little impact on the response variability near fault, but become more pronounced as the fault-to-site distance increases; iii) source effects contribute mostly to the parametric variability at longer periods and are relatively insensitive to both site type and distance. Li and Assimaki [23] also conducted MC simulations of three well-investigated down-hole array sites located in the Los Angeles Basin, using the earthquake dataset developed by Assimaki et.al. [24] based on synthetic records. It was demonstrated that the impact of nonlinear soil property variability depends strongly on the seismic intensity of the applied input motion, particularly in the case of soft soil profiles. In contrast, the effects of velocity profile uncertainties are less intensity dependent and more sensitive

to the velocity impedance in the near surface that governs the maximum site amplification. Similarly, Rathje et.al [25] performed MC simulations for equivalent linear site response analysis by including variability in the bedrock motions, and the elastic and nonlinear soil properties. The statistical model developed by Toro [26] was used to randomise the shear wave velocity profile and the model of Darendeli and Stokoe [7] was implemented to vary the nonlinear soil properties. The results pointed out that modelling shear wave velocity variability generally reduces the predicted median surface motions and amplification factors, most significantly at periods less than the site period, while accounting for the variability in nonlinear properties has a slightly smaller effect. Moreover, including the variability in soil properties significantly increases the standard deviation of the amplification factors but has a lesser effect on the standard deviation of the surface motions.

This paper investigates the influence of the variability in elastic and nonlinear soil properties on the site response prediction of the Large Scale Seismic Test (LSST) site in Lotung, Taiwan. The LSST down-hole accelerometer array has been extensively studied since its establishment by a number of authors[e.g 27, 28, 29, 30, 31, 32, 33, 34], being a well-instrumented benchmark case to test the performance of different numerical approaches in the prediction of site amplification effects. In the great majority of these previous studies, the analysis has been focused on back-analysing some of the recordings of the LSST array using a deterministic approach, while only in the work undertaken by Borja and Sun [33] the sensitivity of the predicted deformation responses to statistical variations of sediment constitutive properties has been considered. Elia et al. [35] attempted to predict the horizontal site response at Lotung using different numerical techniques of increasing level of complexity and adopting, within a deterministic scheme, a single shear wave velocity profile and one set of G/G_0 and D curves for each layer of the soil deposit. In this paper, however, the variability of the elastic and nonlinear soil properties in Lotung is accounted for through a MC approach. Two input motions recorded at the site, one stronger and one weaker, are considered to test the sensitivity of the ground response prediction to the seismic intensity level. The fully-coupled finite element (FE) code SWANDYNE II [36] is adopted and plasticity is introduced in the FE simulations through the advanced elasto-plastic model (RMW) developed by Rouainia and Muir Wood [37]. The performance of the RMW model in fully-coupled dynamic analysis of earth structures has been demonstrated in previous works [e.g. 38, 39].

In the first part of the paper the geological and geotechnical properties of the LSST site are briefly described. The methods adopted in the MC simulations to account for the variability of the initial stiffness profile and soil nonlinear properties shown by the laboratory and in-situ LSST data are

Table 1: Earthquakes recorded by the LSST array and used in the analyses.

Event	Date	Magnitude	Epicentral	Focal	PGA (g) at 47 m			PGA (g) at surface		
		ML	Distance	Depth	N-S	E-W	V	N-S	E-W	V
LSST07	20/5/1986	6.5	66.0	15.8	0.08	0.093	0.03	0.16	0.21	0.04
LSST11	17/7/1986	5.0	6.0	2.0	0.046	0.06	0.015	0.07	0.10	0.044

then discussed and the results of the Lotung nonlinear site response analyses are finally presented.

2. Lotung site and earthquake records

The Lotung accelerometer array is located in the North-East part of Taiwan [40]. The site geology consists of recent alluvium and Pleistocene materials over a Miocene basement. The upper alluvial layer, 30-40 m thick, consists mainly of clayey-silts and silty-clays [41]. The water table is located approximately at a depth of 1 m. The local geological profile (Fig. 1a) shows a 17 m thick silty sand layer above a 6 m thick layer of sand with gravel resting on a stratum of silty clay interlayered by an inclusion of sand with gravel between 29 m and 36 m, as indicated by the SPT log profile reported in Fig. 1b. The site was instrumented in 1985 with down-hole accelerometers located at different depths. Of particular interest here is the vertical array named DHB, which can be considered representative of the free-field response at Lotung. The bedrock formation is assumed to be at a depth of 47 m, where the recordings of the corresponding accelerometer have been used in the numerical simulations as input motions. Between the 1985 and the 1990, 30 earthquakes were recorded with low, moderate and high seismic intensity levels at the LSST site. Two input motions, one strong (LSST07) and one weak (LSST11), have been considered in this work. For the sake of simplicity, only the E-W component of the earthquake events has been adopted in the FE simulations. The LSST11 event was characterised by a shallow focal depth, a smaller epicentral distance, a relatively small magnitude (ML$<$ 5) and peak ground accelerations (PGA) of 0.07 g and 0.10 g respectively in the E-W and N-S direction. On the contrary, the LSST07 event was characterised by a higher magnitude (ML $>$ 5) and maximum accelerations recorded at ground surface equal to 0.16 g and 0.20 g in the E-W and N-S direction, respectively. Among the earthquakes recorded by the Lotung array, the LSST07 event was the second strongest in terms of PGA, while the LSST11 event was one with the lowest magnitude. Table 1 gives general information about the two earthquakes and Fig. 2 shows their acceleration time histories and response spectra at 47 m depth (i.e. bedrock).

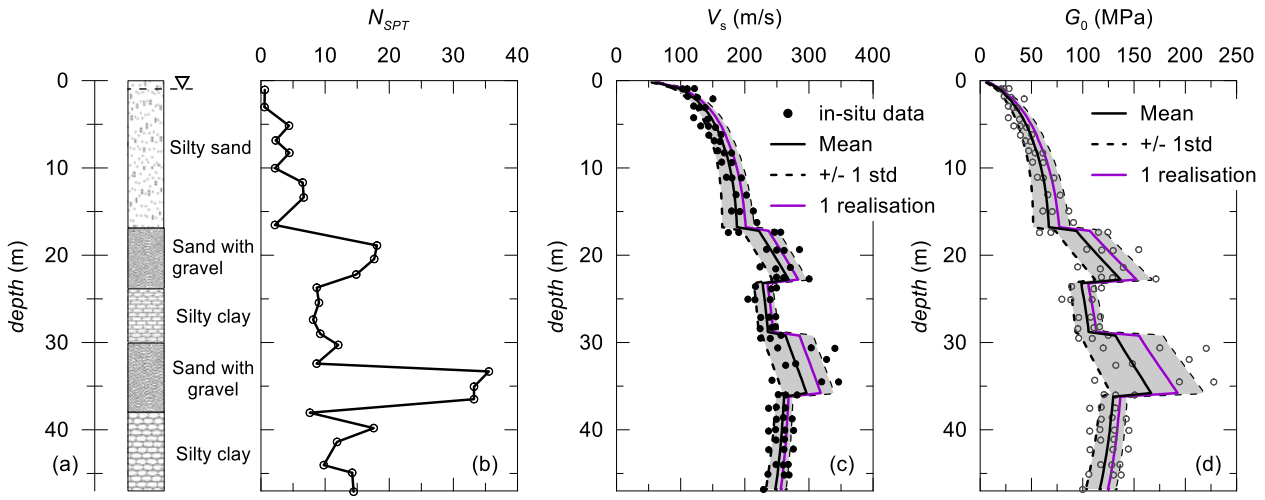

Figure 1: (a) Stratigraphy, (b) SPT log at the LSST site, (c) randomisation of the shear wave velocity profile, (d) randomisation of the initial stiffness profile based on in-situ data (from Anderson and Tang [42] and EPRI [43])

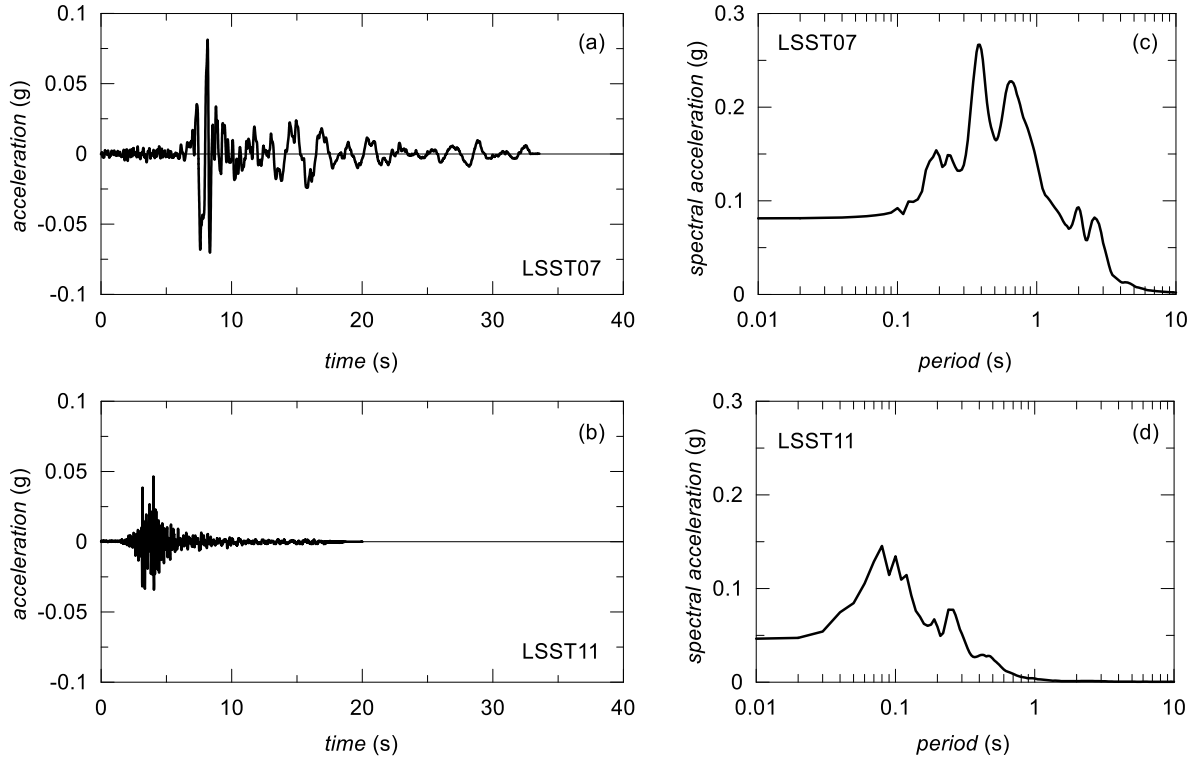

Figure 2: Acceleration time histories and response spectra recorded at the site and adopted in the MC simulations: (a-c) LSST07 and (b-d) LSST11 event.

3. Variability of soil properties

The shear wave velocity profile along with shear modulus reductionand damping curves are the main soil dynamic properties which have significant impact on the response of a site subjected to a specific earthquake event. These properties can vary spatially due to aleatory or epistemic uncertainties. The aleatory uncertainty (or randomness) depends strongly on the site geology and cannot be reduced by the collection of additional information [22]. On the other end, epistemic uncertainty can be caused by man-made errors during laboratory soil testing or deficiencies of current methods in determining the soil properties and can be minimised, for example, by gathering good quality data and developing more rigorous field and laboratory measurement techniques [25]. Most of soil properties are known to exhibit a high coefficient of variation (CV) that can be represented appropriately using a MC method [e.g 23]. In order to randomise the soil properties in each MC simulation, a specific probabilistic distribution for each property is required. However, since the availability of soil data to constrain the selected probabilistic distribution is usually very limited, it is more practical to formulate such distribution based on data from well-monitored and investigated sites.

In this work, the amount of data from the Lotung site, in terms of highquality shear wave velocity measurements and G/G_0 and D laboratory data, allows to undertake MC simulations with well-constrained probabilistic distributions. This is in line with the findings of Teague and Cox [19] and Teague et al. [20] supporting the use of measured data (e.g. surface wave dispersion data and horizontal-to-vertical spectral ratio curves) in the randomisation of the small-strain stiffness profile. The generation of stiffness variability with depth and G/G_0 and D curves for the LSST site is described in the following sections.

3.1. Variability of the initial stiffness profile

The shear wave velocity values obtained at different depths from the results of seismic cross-hole and up-hole tests performed at the LSST site are illustrated in Fig. 2c. The in-situ measurements [42, 43] show a value of about 100 m/s at the surface reaching a value of about 300 m/s at 50 m depth. It is also evident from the in-situ data that the layers consisting in sand with gravel are characterised by distinctively higher V_s values in comparison with the adjacent silty clay and silty sand strata. In the bottom silty clay layer, the V_s data are almost constant or slightly decreasing with depth. Assuming a total unit weight of the soil equal to 20 kN/m^3 (as proposed by Borja et al. [28]), the corresponding values of the small-strain shear modulus, G_0, are reported in Fig. 2d with open dots. The profile of initial stiffness with depth is randomised here, considering the G_0 values

shown in Fig. 2d. To represent the G_0 profile of the Lotung site, the well-known equation proposed by Viggiani and Atkinson [44] is adopted in the FE procedure:

$$\frac{G_0}{p_r} = A\left(\frac{p'}{p_r}\right)R^m \tag{1}$$

where p_r is a reference pressure (equal to 1kPa), p' is mean effective stress, R is overconsolidation ratio and A, m and n are dimensionless stiffness parameters. The details of the FE model and its boundary conditions are presented in Elia et al. [35]. The G_0 profile is described the parameters A, m and n of Eq. 12 and to randomise the small-strain shear modulus profile it is necessary to transfer the variability of G_0 to these parameters. Considering that m and n have relatively less effect on the elastic formulation (due to their small range of values), they are regarded as deterministic input with values of 0.2 and 0.6, respectively. Hence, only the parameter A is subjected to variability when the initial stiffness profile is randomised for the MC simulations. In particular, the initial stiffness profile is varied with a certain standard deviation with respect to a baseline profile. A lognormal distribution of A (and consequently of G_0) can be reasonably fitted through the data points for the different layers, as presented in Fig. 2d. In addition, this assumption provides realistic stiffness profiles as it only generates positive values of G_0 [14]. The mean variation of G_0 with depth shown in the figure corresponds to the profile used to obtain the baseline response.

If the only random parameter in Eq. 12 is A, then the mean, μ_{G_0} , and standard deviation, σ_{G_0}, of G_0 are given by:

$$\mu_{G_0} = \mu_A\left(\frac{p'}{p_r}\right)^n R^m \tag{2}$$

$$\sigma_{G_0} = \sigma_A\left(\frac{p'}{p_r}\right)^n R^m \tag{3}$$

Furthermore, if the mean effective stress and overconsolidation ratio dependency of G_0 is preserved during the calculation of the mean and standard deviation, with the consequence that the CV is held constant during the transformation of A into G_0, it can be shown that the above assumptions result in the following statistical parameters of the lognormal distribution:

$$\mu_{\ln A} = \ln\left(\frac{\mu_A}{\sqrt{1+CV_A^2}}\right) \tag{4}$$

$$\sigma_{\ln A} = \sqrt{\ln\left(1+CV_A^2\right)} \tag{5}$$

Additionally, the log-normally distributed $G_0 \sim (\mu_{\ln G_0}, \sigma_{\ln G_0})$, with the fact that the transformation of variability from A to G_0 only affects the mean of $\ln_{G0}$, thus preserving the standard deviation implies [45]:

$$\mu_{\ln G_0} = \mu_{\ln A} + (1-n)\ln p_r + n \ln p' + m \ln R \tag{6}$$

$$\sigma_{\ln G_0} = \sigma_{\ln A} \tag{7}$$

Once the G_0 profile has been randomised, the corresponding V_s variation with depth is obtained for each realisation (assuming γ = 20 kN/m^3). Fig. 2c displays examples of randomised shear wave velocity profiles used in this study.

3.2. Variability in nonlinear soil properties

The randomisation of the stiffness degradation and corresponding damping curve is, in most cases, based on empirical expressions developed considering different soil types and stress conditions [e.g. 7, 8]. To randomly generate the nonlinear soil parameters, it is necessary to describe their statistical distribution and define any correlation between them. In this work, the G/G_0 and D curves are the output of the RMW model adopted in the simulations. The model consists of three surfaces (Fig. 3). The reference surface controls the state of the soil in its reconstituted, structureless form and describes the intrinsic behaviour of the clay [46]. The structure surface controls the process of destructuration which can be accompanied by significant strain-softening effects. The yield surface (bubble) encloses the elastic domain of the soil. The expression of the reference surface is

$$f_r = \frac{3}{2M_\theta^2}\boldsymbol{s} : \boldsymbol{s} + (p' - p_c)^2 - p_c^2 = 0 \tag{8}$$

where $\boldsymbol{s}$ is the deviatoric stress tensor, p_c is the mean effective stress that defines the size of the reference surface and M_θ is the slope of the critical state line in triaxial space.

The bubble surface is written as

$$f_b = \frac{3}{2M_\theta^2}(\boldsymbol{s} - \boldsymbol{s_\alpha}) : (\boldsymbol{s} - \boldsymbol{s_\alpha}) + (p' - p_\alpha)^2 - (Rp_c)^2 = 0 \tag{9}$$

where $\{p_\alpha \boldsymbol{I}, \boldsymbol{s_\alpha}\}$ denotes the location of the centre of the bubble in the stress space, and accordingly controls its kinematic hardening, $\boldsymbol{I}$ is the second-order identity tensor, and R is the size of the bubble relative to the structure surface.

The structure surface is given by

$$f_s = \frac{3}{2M_\theta^2}\big[\boldsymbol{s} - (r-1)\boldsymbol{\eta}_0 p_c\big] : \big[\boldsymbol{s} - (r-1)\boldsymbol{\eta}_0 p_c\big] + (p' - r p_c)^2 - (r p_c)^2 = 0 \tag{10}$$

where $\boldsymbol{\eta}_0$ is a fixed deviatoric tensor controlling the structure and r represents the progressive degradation of the material. For more details on the formulation and implementation of the RMW model the reader is referred to Rouainia and Muir Wood [37, 47] and Zhao et al. [48].

The constitutive law allows to reproduce some of the key features of the cyclic behaviour of natural soils, such as the destructuration induced by the loading, the decay of the shear stiffness with strain amplitude, the corresponding increase of hysteretic damping and the accumulation of excess pore water pressure under undrained conditions. A kinematic hardening translation rule is used to model the movement of the centre of the yield surface, $\boldsymbol{\alpha}$, in a direction parallel to the line joining the current stress, $\boldsymbol{\sigma}$, and the conjugate stress, $\boldsymbol{\sigma_c}$, as follows:

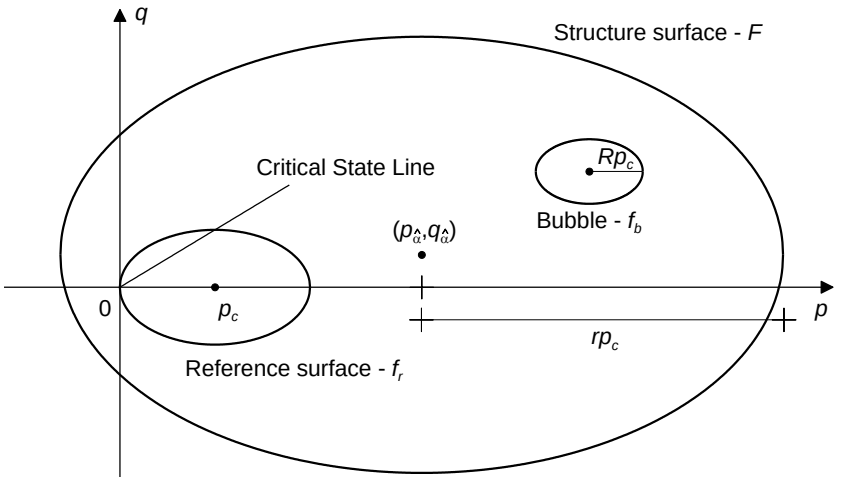

Figure 3: Schematic representation of the RMW model in the (p', q) plane

$$\dot{\boldsymbol{\alpha}} = \boldsymbol{\alpha}\left(\frac{\dot{p}'}{p_c} + \frac{\dot{r}}{r}\right) + \dot{\mu}\big(\boldsymbol{\sigma_c} - \boldsymbol{\sigma}\big) \tag{11}$$

where μ is a positive scalar of proportionality, p_c is the mean effective stress that defines the size of the reference surface and r is the degree of structure, which is a monotonically decreasing function of the plastic strain. It should be noted that the centre of the structure surface represents the anisotropy of the soil due to structure. The plastic modulus H is assumed to depend on the distance between

the current stress and the conjugate stress and is given by:

$$H = H_c + \frac{Bp_c^3}{\lambda^* - \kappa^*}\left(\frac{b}{b_{max}}\right)^{\psi} \tag{12}$$

where λ^* and κ^* are the slopes of normal compression and swelling lines in the $\ln v - \ln p'$ compression plane (v is the soil specific volume), $b = \bar{\boldsymbol{n}} : (\boldsymbol{\sigma_c} - \boldsymbol{\sigma})$ is a measure of the distance between the yield and the structure surface and b_{max} is the nominal maximal value of b. The additional soil parameters ψ and B control the rate of decay of stiffness with strain and the magnitude of the contribution of the interpolation term, respectively. The hardening modulus H_c is derived from the consistency condition on the structure surface when the yield and the structure surface are in contact.

Fig. 4 presents the comparison between the stress-strain timehistories estimated by Zeghal et al. [49] processing the accelerations recorded during the LSST16 event and those predicted at the same depths during the LSST07 event using RMW with baseline parameters. The LSST16 earthquake was characterised by a local magnitude of 6.8 and a focal depth of 15 km, with values of the peak ground acceleration very similar to those of the LSST07 event. The results shown in Fig. 4 represents a validation of the advanced RMW analyses, highlighting the good performance of the model to properly capture the observed continuous change of stiffness and damping properties throughout the motion.

The randomisation of the soil nonlinear parameters can be achieved by varying the RMW parameters which mostly affect the predicted stiffness degradation and damping curves. To identify these parameters, a series of single element simulations of strain-controlled undrained cyclic simple shear (CSS) tests are conducted by applying different shear strain amplitudes. After 500 cycles for each strain level, which is considered to be sufficient to achieve a steady-state condition [50], the secant shear modulus and damping ratio values are obtained. From an extensive parametric study, it is observed that the G/G_0 and D curves are greatly affected by the interpolation exponent ψ in Eq. 6. The soil parameter ψ is, then, considered as log-normally distributed between a lower value of 0.1 and an upper value of 4. The range of ψ values is determined in order to reasonably capture the variability of the torsional shear and resonant column laboratory measurements performed on undisturbed soil samples from Lotung [43] and the data back-figured by Zeghal et al. [49], both presented in Fig. 5. It should be noted that the back-calculated values of G/G_0 and D show a higher variability than the laboratory data. Nevertheless, previous works on Lotung [31] have identified in the variations of the moduli and damping ratios with shear strain, rather than the variability of the measured shear wave velocities, the greatest source of uncertainty. Therefore, both sets of G/G_0

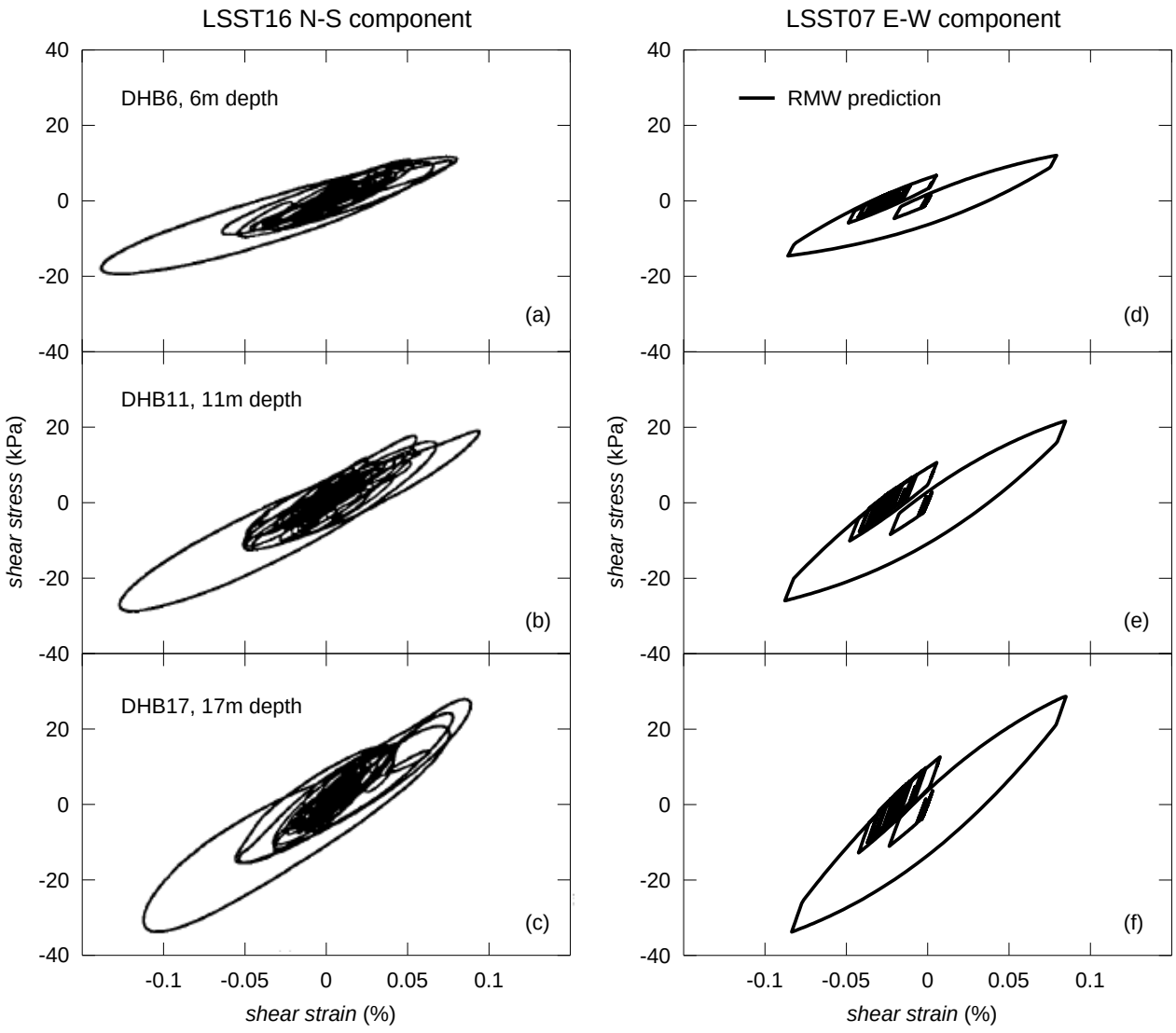

Figure 4: Comparison between stress-strain histories obtained (a-c) by Zeghal et al. [49] for the LSST16 event and (d-f) using RMW during the LSST07 event.

Table 2: RMW material parameters for the different soil layers used in the analyses.

Depth	λ^*	κ^*	M	R	B	ψ	r_0	A	m	n
0-17 m	0.044	0.015	0.922	0.085	1.0	varied	1.0	varied	0.2	0.6
17-23 m	0.044	0.015	1.096	0.085	1.0	varied	1.0	varied	0.2	0.6
23-29 m	0.044	0.015	0.814	0.085	1.0	varied	1.0	varied	0.2	0.6
29-36 m	0.044	0.015	0.941	0.085	1.0	varied	1.0	varied	0.2	0.6
36-47 m	0.044	0.015	0.730	0.085	1.0	varied	1.0	varied	0.2	0.6

and D data are considered in the analysis presented in this paper. The mean value of the parameter ψ is set equal to 1.0, as this assumption, along with the remaining soil parameters, gives the baseline nonlinear curves adopted in previous deterministic studies [35]. The CV of ψ is assumed equal to 0.4, in accordance with the guidance given in the literature [e.g 9, 51]. Random ψ values are generated such that they are within the lower and upper limit. The corresponding range of G/G_0 and D curves obtained through CSS simulations with the RMW model are shown in Fig. 5. A small amount of viscous damping, equal to 3%, is introduced into the FE model through a standard Rayleigh formulation [52] to compensate for the RMW underestimation of damping within the small-strain range. The smaller ψ value gives the stiffer G/G_0 reduction with shear strain and thus leads to the lower damping curve. In contrast, for the largest value of ψ the RMW model predicts a more rapid stiffness degradation, resulting in higher hysteretic damping. This inverse trend of the predicted G/G_0 and D curves showsthe RMW model is able to automatically replicate the well-known negative correlation between the two curves. Table 2 summarises the RMW parameters adopted in the MC simulations. The critical state stress ratio value for each soil layer corresponds to the effective friction angle back-calculated from the SPT data reported in Fig. 2b and is assumed fixed in the analyses. It should be also noted that the adopted value of the parameter R, which represents the ratio of the sizes of the elastic bubble and the reference yield surface, is very small in order to capture the early stiffness degradation at small strains shown by the LSST soils (see Fig. 5). This assumption in the model calibration implies a prediction of a highly nonlinear cyclic behaviour over a wide range of seismic induced strains, which has a strong influence on the MC results described in the following section.

4. Results and discussion

In this section, the results of MC simulations of Lotung nonlinear siteresponse are presented in terms of median response spectrum predicted at ground surface and compared with the actual

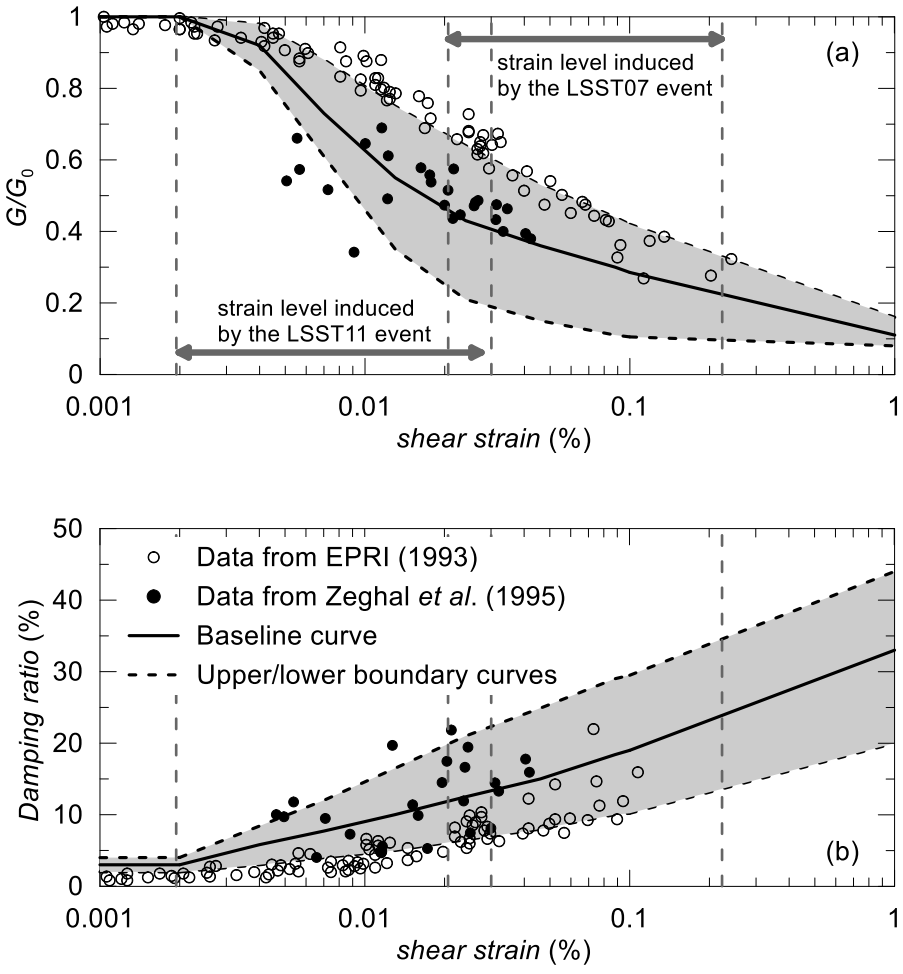

Figure 5: Randomisation of the (a) normalised stiffness degradation and (b) damping curves, based on laboratory results ([43] 1993) and back-figured data by Zeghal et al. [49].

LSST recorded data and the response spectra computed by Elia et al. [35] for the best-estimate soil properties (baseline response) using a deterministic approach. The influence of initial stiffness and nonlinear soil property variability is investigated for both the strong and the weak input motion. The figures show the results obtained using 200 stiffness (V_s) or, alternatively, 200 nonlinear curves (G/G_0) realisations. The simultaneous variability of the V_s profile and nonlinear curves is also considered. To accurately assess the site response predictions, the standard deviation of the logarithmic spectral accelerations, $\sigma_{\ln S_a}$, is plotted, as proposed by Li and Assimaki [23] and Rathje et al. [25].

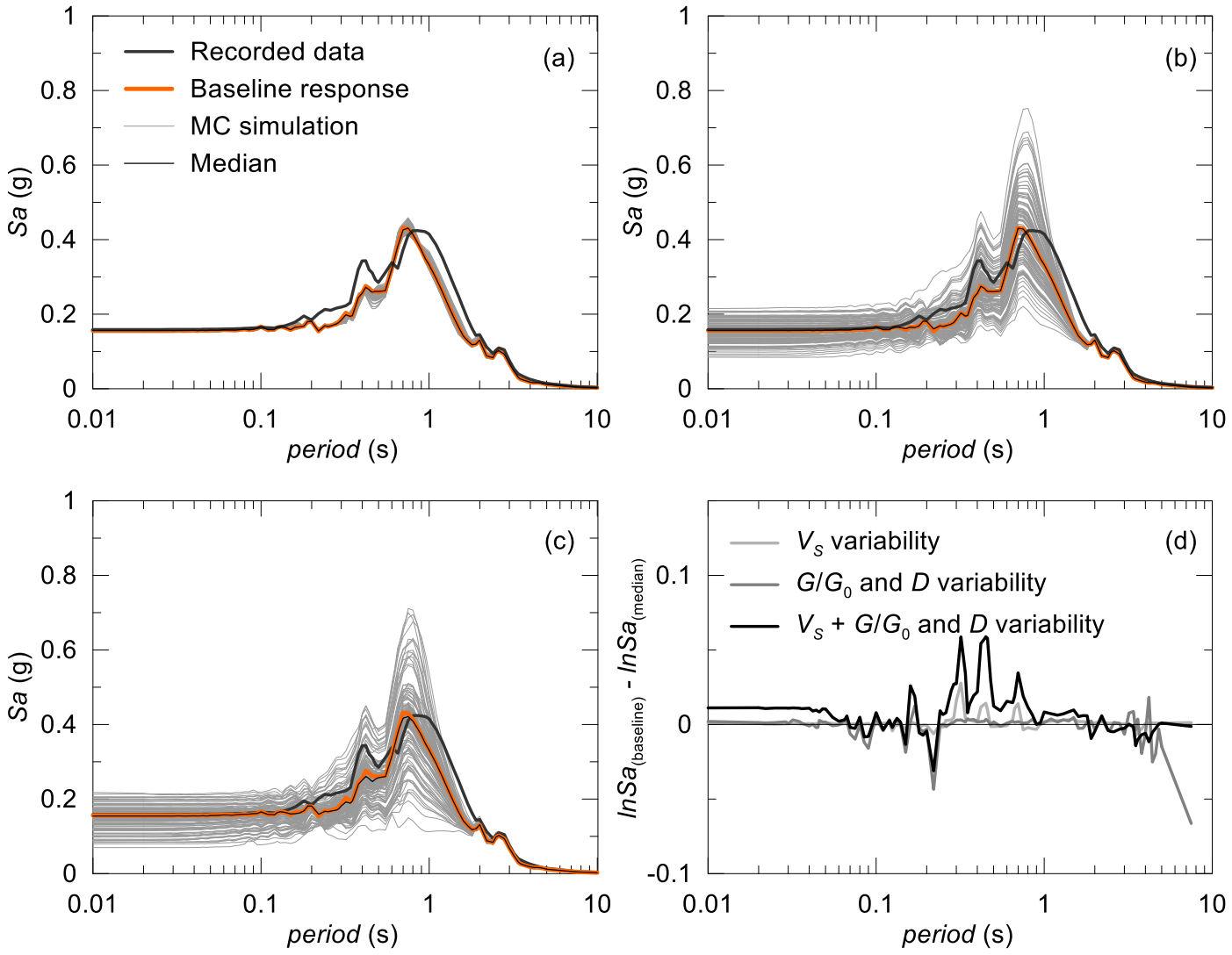

Figure 6: Influence on the site response prediction for the LSST07 event of (a) stiffness profile, (b) nonlinear curves variability, (c) simultaneous variability of V_s profile and nonlinear curves and (d) spectral residuals.

4.1. Effects of soil property variability on LSST site response during the stronger input motion

The surface response spectra of the nonlinear site response analyses when the strong input motion (LSST07) is applied at bedrock are shown in Fig. 6. The results are obtained with the V_s profile and G/G_0 and D curves being randomised around the baseline within $\pm$ one standard deviation. Different levels of truncation around the baseline (i.e. adding $\pm$ two and three standard deviations) are also considered. By statistically changing the V_s profile, the MC simulations clearly exhibit only a modest variation in the response spectra at surface over the engineering period of interest (Fig. 6a). Moreover, the median is remarkably similar to the baseline response prediction. This is confirmed by the plot of residual spectral accelerations (i.e. the difference between the baseline and MC median logarithmic spectral accelerations) presented in Fig. 6d. In contrast, a significant variation in the response spectra can be observed by randomising the G/G_0 and D curves, keeping the V_s profile unchanged (Fig. 6b). The median, in this case, also closely matches the baseline response (Fig. 6d). As a third possible case, the V_s profile and the nonlinear curves are randomised simultaneously (Fig. 6c), leading to standard deviation values higher than those obtained by changing the G/G_0 and D curves only.

The median surface response obtained for one, two and three standard deviation level of truncation around the V_s baseline profile is presented in Fig. 7, while the effect of changing the truncation level of the G/G_0 and D curve distributions is shown in Fig. 8. As the standard deviation around the V_s profile is increased from one to three, no appreciable effect on the median response spectra at the surface can be observed, resulting in an identical degree of uncertainty in terms of $\sigma_{\ln S_a}$. In contrast, increasing the level of truncation of the G/G_0 and D distributions causes high variability in the standard deviations of the logarithmic spectral accelerations at surface, but the median response remains almost unchanged.

The greatest influence of nonlinear curves variability, compared to that of the initial stiffness profile, on the site response predictions during the LSST07 event is confirmed by the results of maximum horizontal acceleration and shear strain profiles, shown in Fig. 9. The comparison between Figs. 9a and Fig. 9c, where the acceleration data recorded at the LSST site are also reported, clearly highlights the higher influence of $G/G0$ and D variability, with respect to the initial stiffness profile, on the maximum accelerations predicted at different depths. In both cases, the median profile is, nevertheless, very similar to the baseline prediction. Moreover, the variation of shear wave velocities implies a variability of the induced shear strains between 0.05% and 0.13% (Fig. 9b), with maximum standard deviation of 0.011% at 15 m depth, while the variability associated to the variation of the

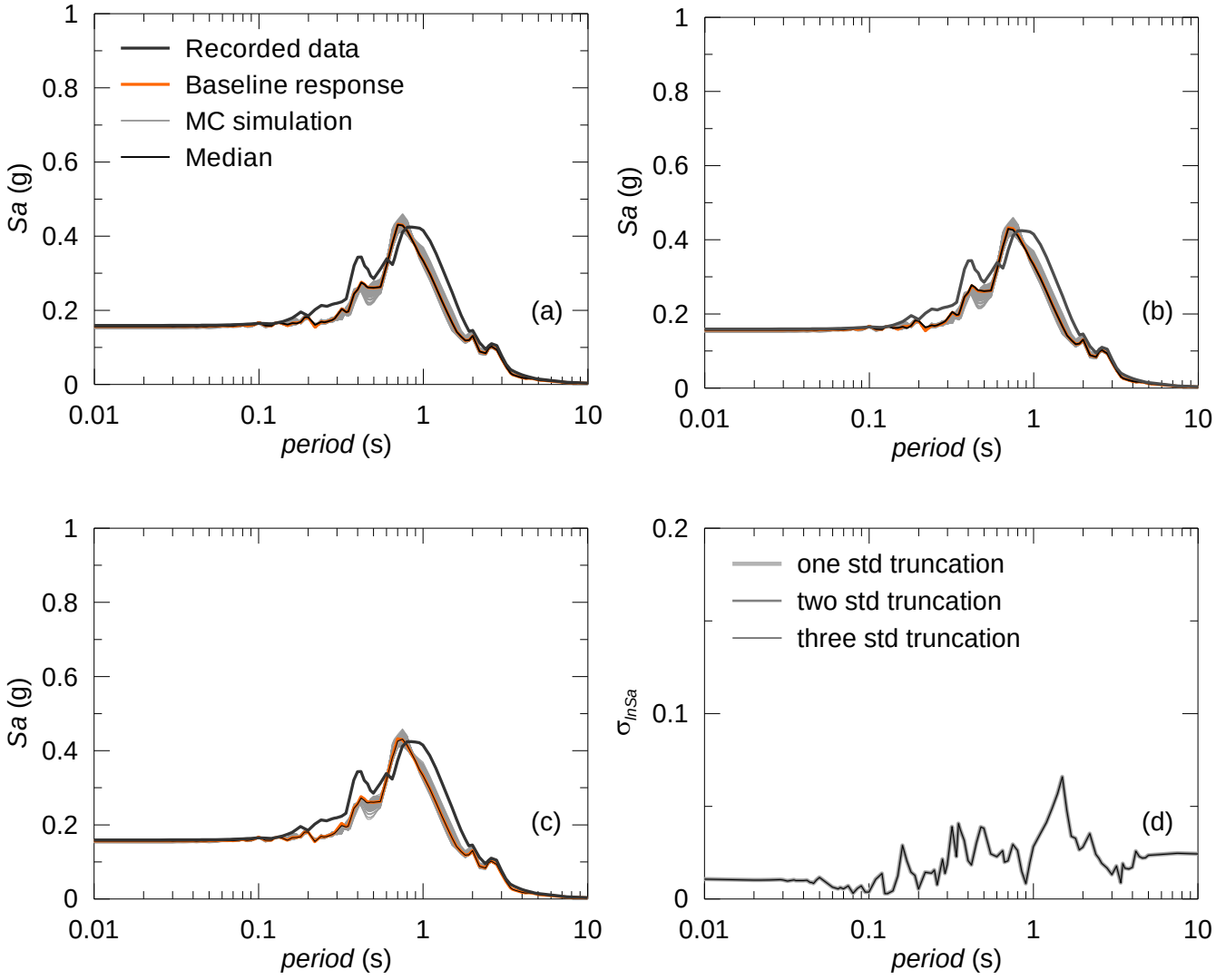

Figure 7: Median surface response observed during the LSST07 event for (a) one, (b) two, (c) three standard deviation level of truncation around the Vs baseline profile and (d) standard deviation of the surface response spectra.

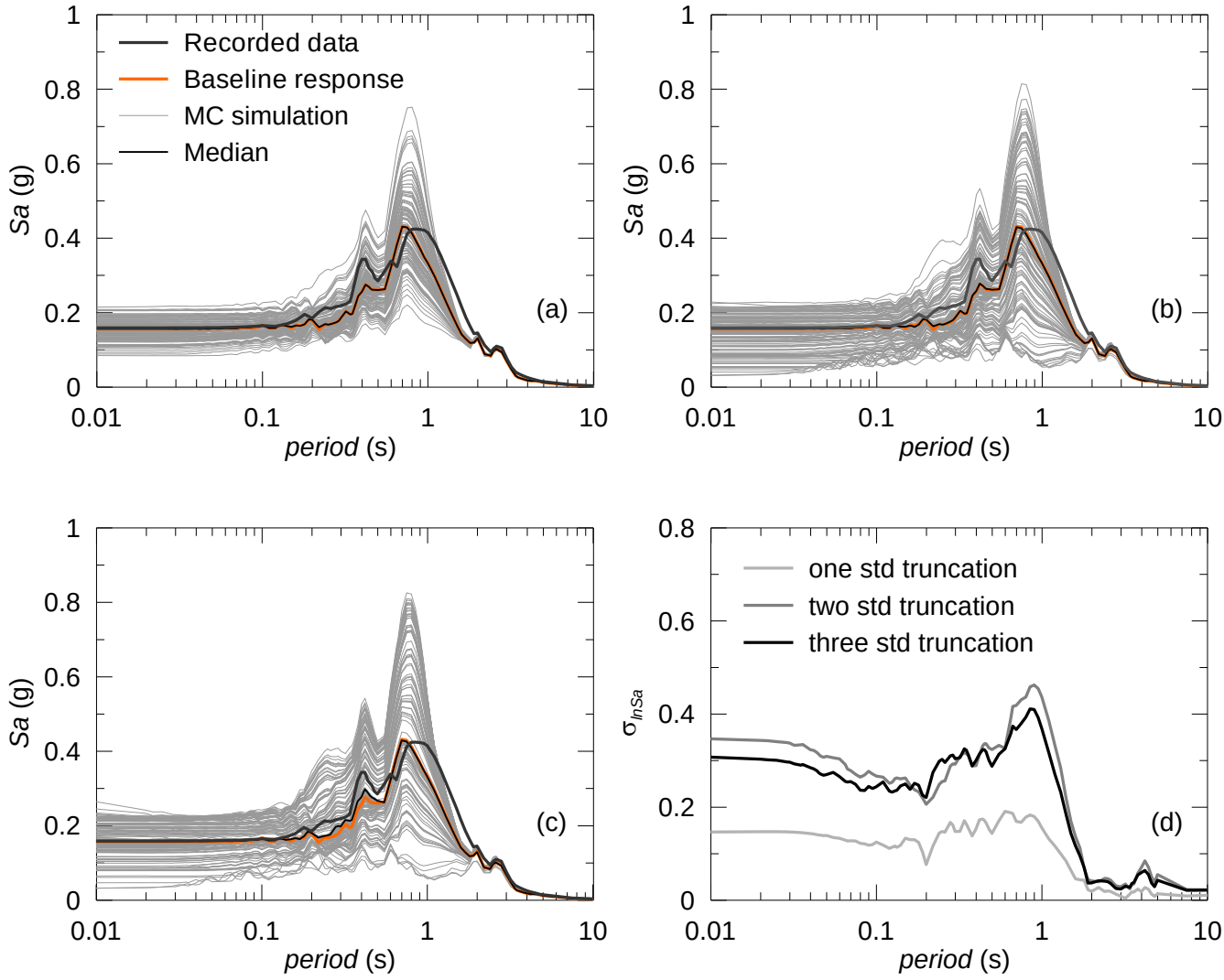

Figure 8: Median surface response observed during the LSST07 event for (a) one, (b) two, (c) three standard deviation level of truncation around the G/G_0 and D curves and (d) standard deviation of the surface response spectra.

moduli and damping ratios is much higher, especially in the top 10 meters (Fig. 9d), ranging between 0.02% and 0.22%, with maximum standard deviation of 0.029% at 9 m depth. This level of shear strain (i.e. 0.02-0.22%) is sufficient to cause a nonlinear soil behaviour in conjunction with a considerable reduction of the initial shear modulus and corresponding increase of damping ratio (as can be seen in Fig. 5). This is due to the very small size of the elastic domain assumed in the RMW calibration (Table 2).

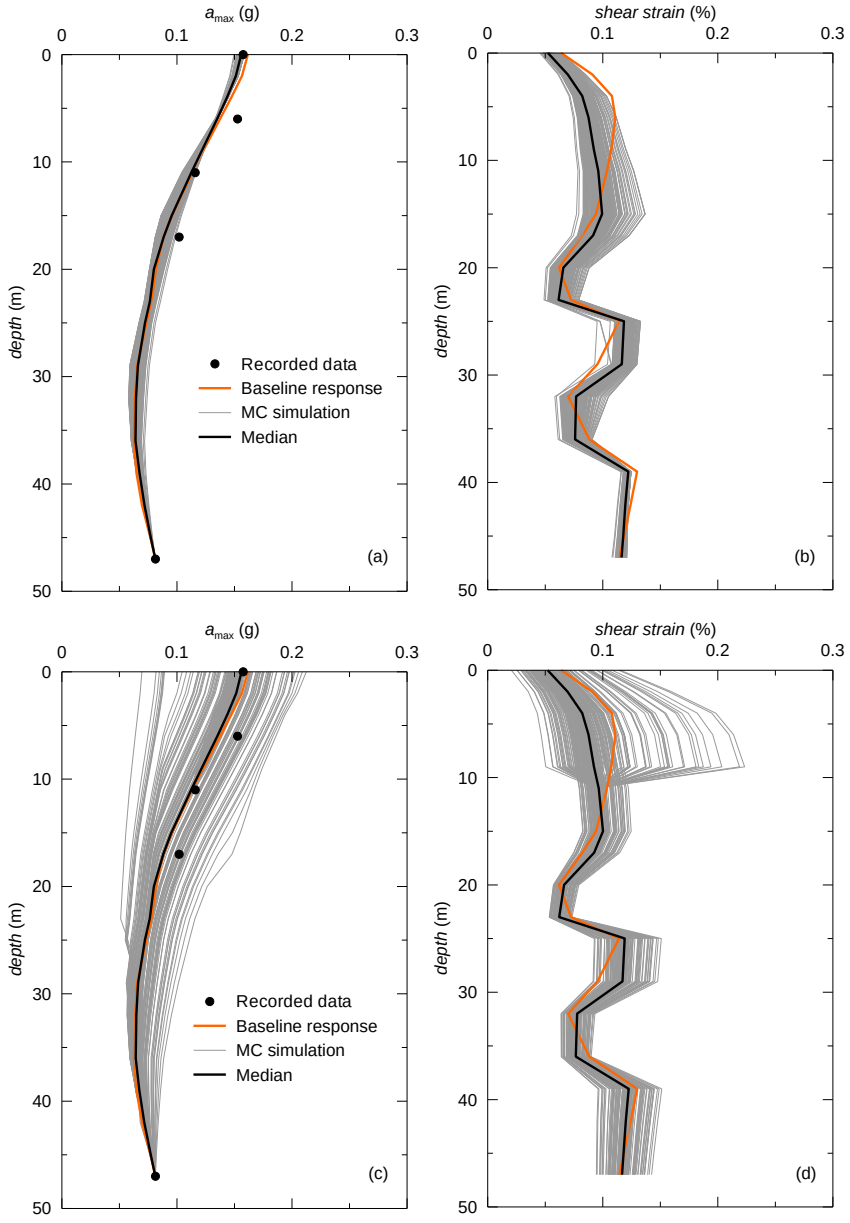

Figure 9: Influence of (a-b) stiffness profile and (c-d) nonlinear curves variability on the maximum horizontal acceleration and shear strain profiles for the LSST07 event.

Finally, to estimate the number of MC simulations required to achieve a consistent site response

prediction, when the G/G_0 and D curves are varied, five suites of 10, 20 and 50 realisations are considered. Each suite represents a reasonable realisation of nonlinear curves, such that the comparison between the results of different suites provides an evaluation of the statistical stability of the computed response. This analysis is not performed for the shear wave velocity profile, as the MC simulation results presented in Fig. 6a show that the spectral response at surface of 200 different realisations of V_s exhibit inconsiderable level of dispersion around the baseline prediction. The median surface response spectrum and the standard deviation of the surface response spectra ($\sigma \ln S_a$) at each period are computed for each suite of G/G_0 and D curves and plotted in Fig. 10. It is clear how 10 and 20 realisations do not produce a consistent median response at surface. In contrast, using 50 realisations allows to predict a stable response, very close to the baseline prediction (Fig. 10c). This is also evident in Fig. 10d, where the reduction of the standard deviation as the number of realisations increases from 10 to 50 is presented. At the lower periods, sets of 10 and 20 realisations have similar but higher values of standard deviation with respect to the suite composed by 50 realisations, while the difference becomes evident at around 0.85 s, representing the first natural period of the column (T_1). This can be explained by the tendency of the system to oscillate around its fundamental period, leading to substantial spectral amplifications at this period. Therefore, the spectral response predictions become more sensitive to the variability of the soil properties at around T_1, causing great deviations in the results. At the higher periods (greater than 2 s), the standard deviations of the suites composed by 20 and 50 realisations are very similar.

4.2. Effects of soil property variability on LSST site response during the weaker input motion

An analogous statistical analysis is conducted applying the LSST11motion at bedrock. Fig. 11 describes the influence of stiffness profile and nonlinear curves variability on the site response prediction in this case. The variation of the V_s profile has now a significant impact on the site response prediction at the surface (Fig. 11a). The median response spectrum obtained from the MC simulations is greater than the baseline result for periods below 0.35 s and smaller at T_1, as observed from the spectral residual plot shown in Fig. 11d. In contrast, there is almost no influence of the variability of the G/G_0 and D curves on the response at surface, as can be seen in Fig. 11b showing an exact match between each MC simulation and the baseline spectral prediction (Fig. 11d). Consequently, the standard deviation of the logarithmic spectral accelerations is equal to zero for each period. If the initial stiffness profile and the nonlinear curves are randomised simultaneously, the predictions are not particularly different from those obtained by changing the V_s profile only (Fig. 11c), with slightly higher spectral residuals at the lower periods (Fig. 11d).

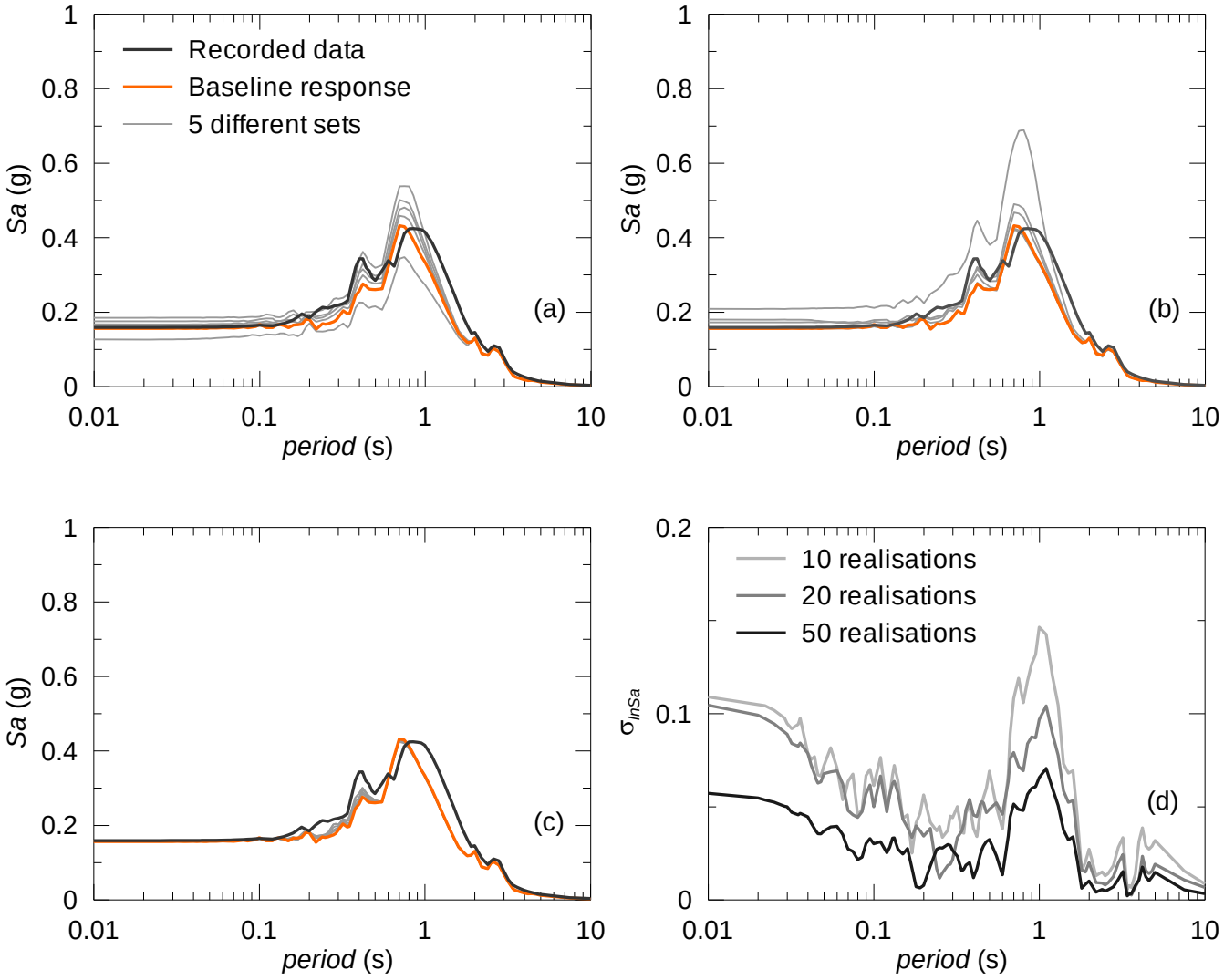

Figure 10: Median surface response observed during the LSST07 event for suites of (a) 10, (b) 20, (c) 50 realizations of nonlinear curves and (d) standard deviation of the surface response spectra.

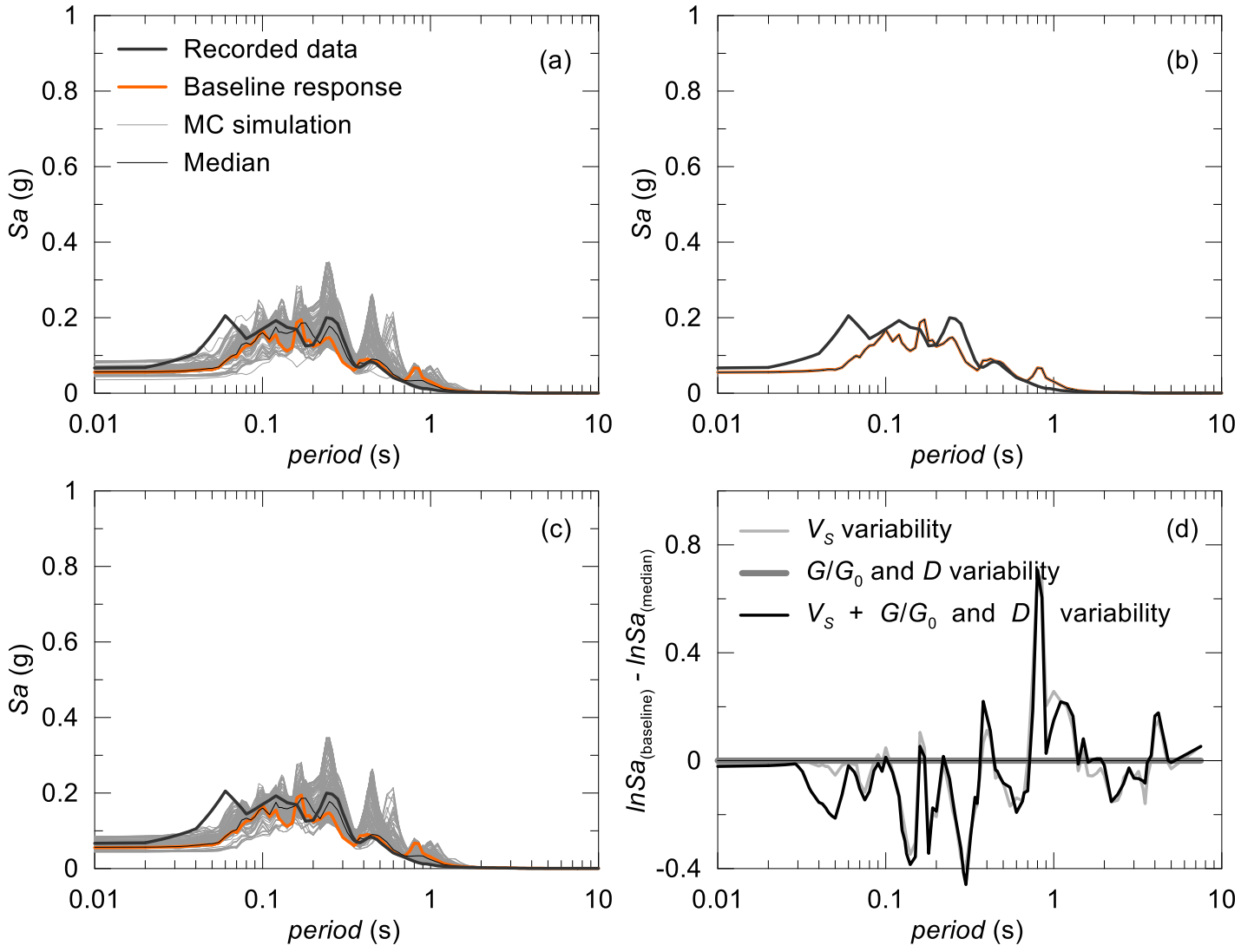

Figure 11: Influence on the site response prediction for the LSST11 event of (a) stiffness profile, (b) nonlinear curves variability, (c) simultaneous variability of V_s profile and nonlinear curves and (d) spectral residuals.

Fig. 12 presents the median surface response obtained for one, two and three standard deviation level of truncation around the V_s baseline profile. The consideration of a wide range of variability of the V_s profile by increasing the level of truncation leads to an improvement in the response prediction at the surface. Actually, the predicted median response spectrum becomes almost identical to the recorded data for periods higher than 0.2 s when two standard deviations are considered (Fig. 12b). No further improvements with respect to the recorded accelerations can be obtained increasing the truncation level to three standard deviations (Fig. 12c). At the same time, the logarithmic standard deviation of the spectral accelerations increases with the rise of the truncation level (Fig. 12d). Therefore, considering two or three standard deviation levels of truncation around the V_s baseline profile can result in a slightly better prediction at surface, but this requires more site response analyses to obtain the same level of stability in the simulation results. On the contrary, the change in the truncation level around the G/G_0 and D curve distributions does not introduce appreciable changes or variability in the response prediction, as shown in Fig. 13, thus confirming the results presented in Fig. 11b. The site response is, in fact, more sensitive to the initial stiffness profile when the weaker motion is applied at bedrock, as the level of shear strain induced by the earthquake is, in this case, relatively small.

To prove this idea, Fig. 14 presents the influence of stiffnessprofile and nonlinear curves variability on the maximum horizontal acceleration and shear strain profiles for the LSST11 event. The variation of the initial stiffness profile implies a variability of the induced shear strains between 0.002% and 0.03% (Fig. 14b), with maximum standard deviation of 0.006% at 6 m depth. This level of shear strains induced by the weaker motion (i.e. 0.002-0.03%) is reported in Fig. 5, and results to be almost one order of magnitude lower than that associated to the LSST07 event, thus justifying the higher sensitivity to the V_s variability in the LSST11 case. In contrast, the shear strain variability associated to the variation of the moduli and damping ratio is almost negligible (Fig. 14d). The median profile of amax is closer to the Lotung data recorded along the depth when the variation of the V_s profile is accounted for (Fig. 14a), while the variability of the G/G_0 and D curves has almost no effect on the MC simulation results in terms of maximum acceleration profile (Fig. 14c), consistently with the results shown in Fig. 11.

Since the V_s profile is the main factor controlling the predictedspectral accelerations when the weaker input motion is considered, the adequate number of initial stiffness profile realisations required to get a consistent response at the surface is investigated. Fig. 15 presents the median response spectra for five sets of 10, 20 and 50 realisations of V_s and their standard deviations. The

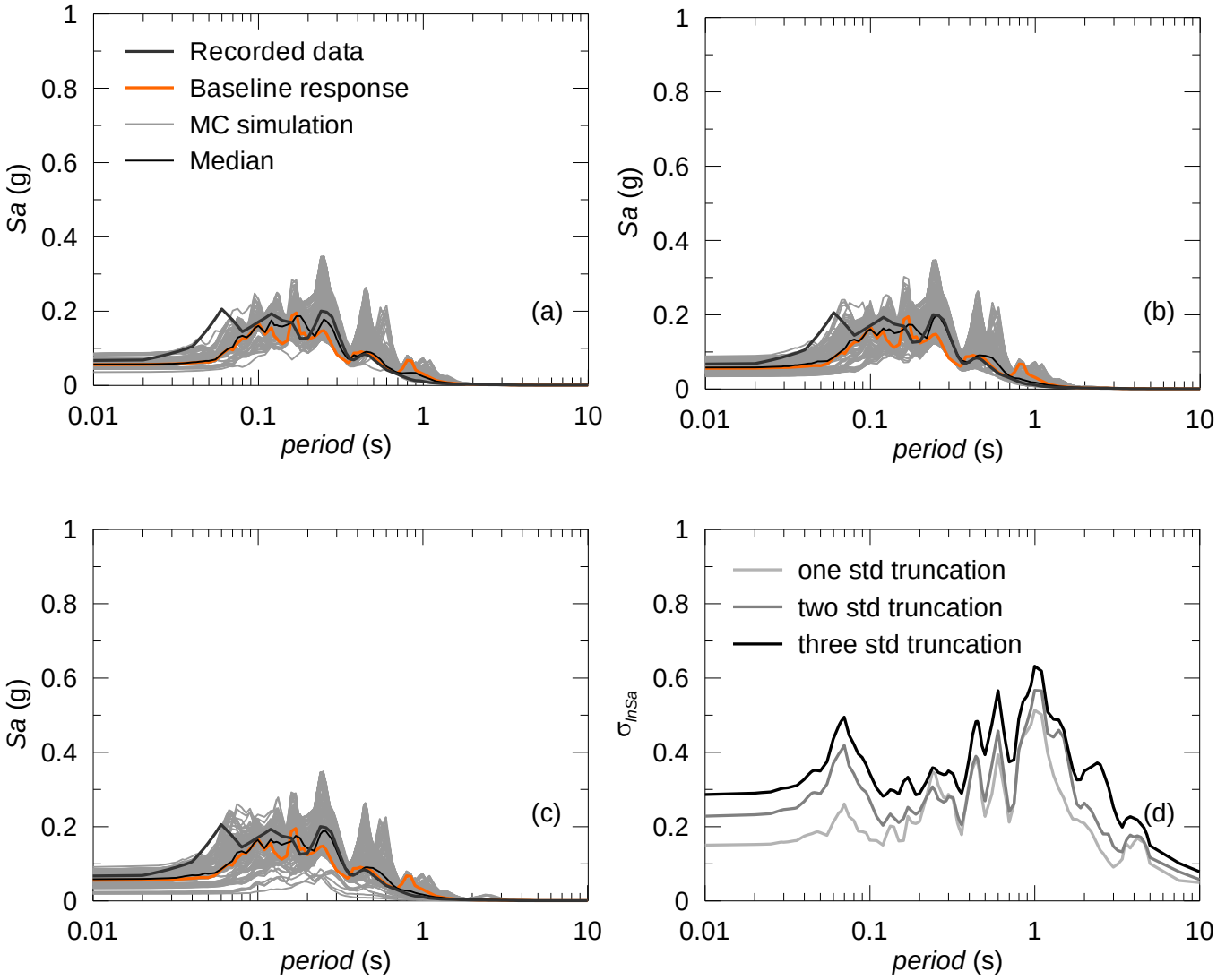

Figure 12: Median surface response observed during the LSST11 event for (a) one, (b) two, (c) three standard deviation level of truncation around V_s baseline profile and (d) standard deviation of the surface response spectra.

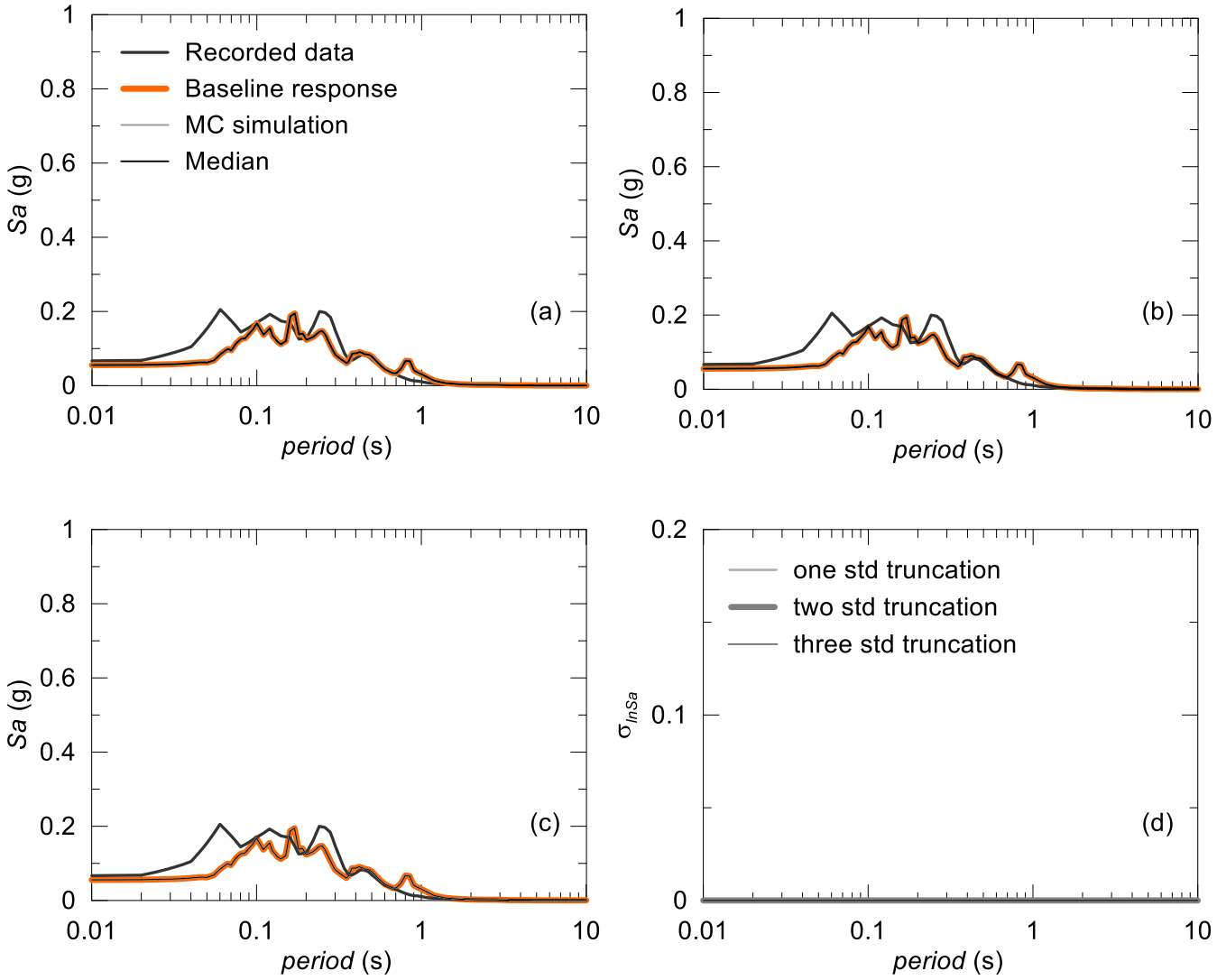

Figure 13: Median surface response observed during the LSST11 event for (a) one, (b) two, (c) three standard deviation level of truncation around G/G_0 and D curves and (d) standard deviation of the surface response spectra.

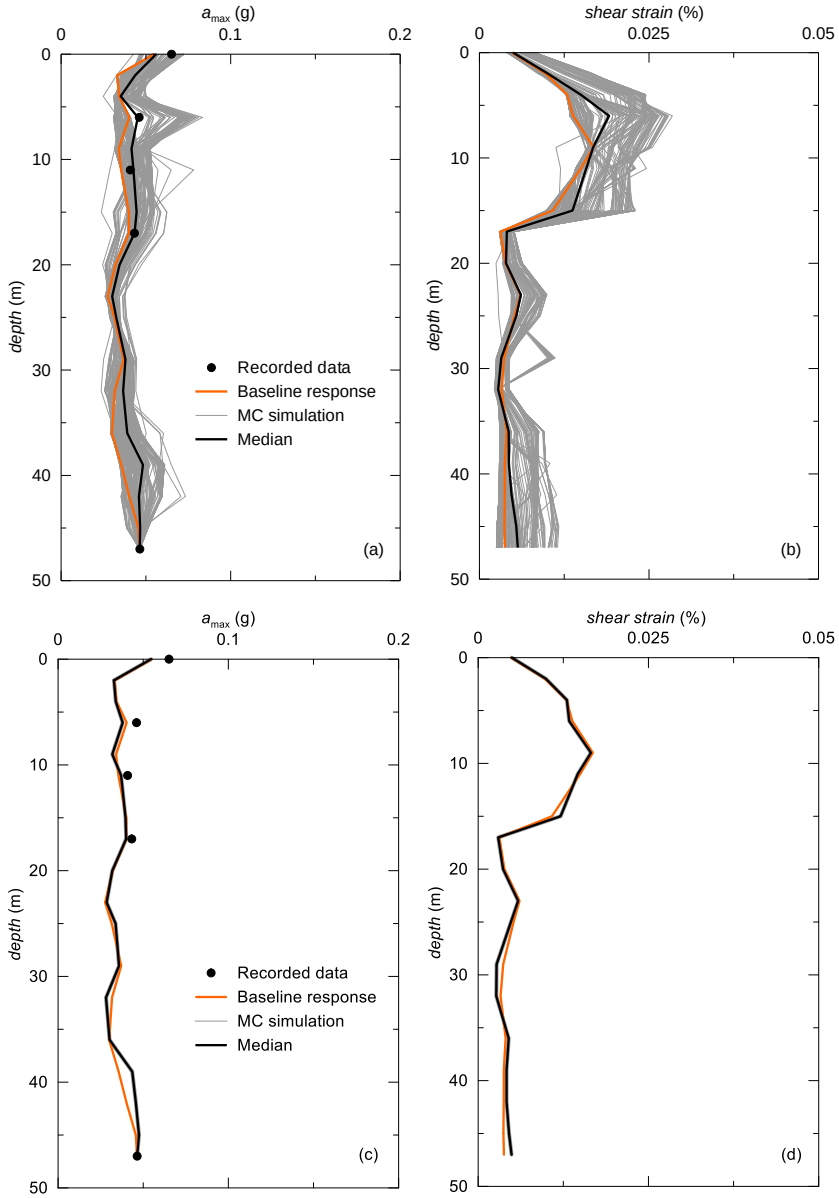

Figure 14: Influence of (a-b) stiffness profile and (c-d) nonlinear curves variability on the maximum horizontal acceleration and shear strain profiles for the LSST11 event.

suites of 10 or 20 realisations produce a significant variation in the median responses (Figs. 15a and 15b). Conversely, the set of 50 realisations reduces the variability of the median responses, particularly in the period range between 0.3 s and 2 s, as shown in Fig. 15c. This ensures the prediction of a surface response characterised by less variability. When a suite of 50 realisations is considered, some discrepancies between the median spectral values can be still observed, but the level of standard deviation is considerably reduced (Fig. 15d).

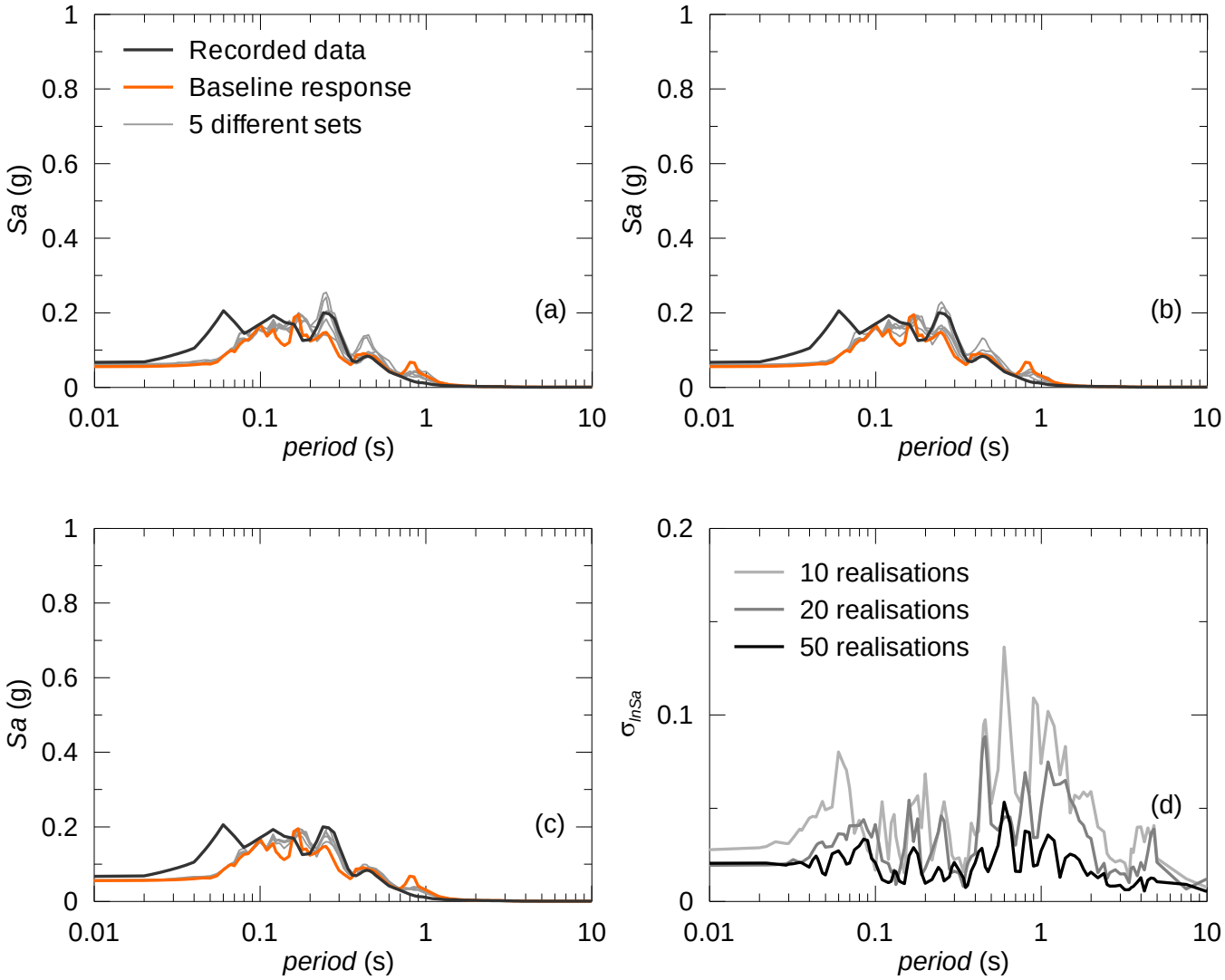

Figure 15: Median surface response observed during the LSST11 event for suites of (a) 10, (b) 20, (c) 50 realizations of V_s profile and (d) standard deviation of the surface response spectra.

5. Conclusion

This study investigates the influence of variability of elastic andnonlinear soil properties (i.e. shear wave velocity profile, shear modulus reduction and damping curves) on site response predictions through a Monte Carlo approach. For this purpose, the Large Scale Seismic Test site in Lotung is back-analysed using a fully-coupled finite element code and plasticity is introduced in the simulations through a kinematic hardening soil model. Two different input motions recorded at the site, one weaker and one stronger, are applied at bedrock to investigate the sensitivity of the statistical results to the seismic intensity level. The outputs of the MC simulations are interpreted in terms of spectral responses at surface and standard deviation of the logarithmic spectral accelerations. They are also compared to the recorded array data available at the site and to the baseline predictions of deterministic FE analyses performed adopting best-estimate soil properties.

Overall, the results of the statistical approach indicate that, in the specific Lotung case, the effect of variability in the elastic and nonlinear soil properties on the site response predictions shows a great dependency on the seismic intensity level of the input motion. In the case of a stronger motion, the spatial variability of the stiffness degradation and damping curves has a more pronounced effect on the predicted LSST site response, as nonlinearity is triggered by the high level of induced shear strains. Nevertheless, the median response spectrum of the MC simulations is remarkably similar to the baseline prediction, even if the level of truncation is increased. In contrast, the MC results at surface are particularly sensitive to the statistical variation in the initial stiffness profile when a weaker motion is considered, as nonlinear effects are negligible in this case. The novelty of the work is represented by the clear separation between the effect of stiffness variability and that of soil nonlinear properties on the MC simulation results obtained with the advanced kinematic hardening model. Previous studies have, in fact, shown a more pronounced influence of V_s variability on ground response predictions, even when large strains are induced by high intensity motions. With respect to this point, it should be noted that:

- this is one of the first attempt to use an advanced soil constitutive model in nonlinear MC simulations of ground response, as much simpler constitutive assumptions are usually adopted in this type of statistical investigations;
- The advanced constitutive model employed in this paper is characterised by a very small elastic domain, thus simulating a mechanical behaviour of the LSST soils dominantly controlled by the soil nonlinear properties over a wide range of seismic induced strains. A more evident influence of the initial stiffness variability could be obtained with the advanced nonlinear approach in other

case studies where the stiffness degradation data indicate a larger yield surface enclosing the elastic soil behaviour.

Finally, this work complements the results obtained by Elia et al. [35] for the same case study, which has highlighted the importance of the shear wave velocity profile in the top layers of the LSST deposit on the prediction of the accelerations recorded at surface. The results of the FE simulations can be highly affected by the stiffness contrast between adjacent layers and the thickness adopted in the modelling for each soil layer. Although the spatial stiffness variability implemented in this study can be considered as a random characterisation of the stiffness contrast between layers, further research is still required on this aspect of the work.

Acknowledgments The first author was funded by a studentship grant from the Ministry of National Education, Republic Turkey. This support is gratefully acknowledged. The authors would also like to thank Tom Charlton for his valuable input into the representation of soil variability.

References

[1] Kramer SL. Geotechnical Earthquake Engineering. Prentice Hall, Upper Saddle River, N.J; 1996.

[2] Roesset JM. Soil amplification of earthquakes. In Desai and Christian editors. Numerical Methods in Geotechnical Engineering, McGraw-Hill; 1977, p. 639-682.

[3] Kaklamanos J, Baise LG, Thompson EM, Dorfmann L. Comparison of 1D linear, equivalent-linear, and nonlinear site response models at six KiK-net validation sites. Soil Dyn Earthq Eng 2015;69:207-219.

[4] Zalachoris G, Rathje EM. Evaluation of one-dimensional site response techniques using borehole arrays. J Geotech Geoenviron 2015;141(12):04015053.

[5] Elia, G. (2015) Site response for seismic hazard assessment, In: Encyclopedia of Earthq Eng - Springer (DOI: 10.1007/978-3-642-36197-5_241-1).

[6] Vucetic M, Dobry R. Effects of the soil plasticity on cyclic response. J Geotech Eng-ASCE 1991; 117(1):89-107.

[7] Darendeli MB, Stokoe KH. Development of a new family of normalized modulus reduction and material damping curves. Geotech. Engrg. Rpt. GD01-1, University of Texas, Austin, Texas; 2001.

[8] Zhang J, Andrus RD, Juang CH. (2005) Normalized shear modulus and material damping ratio relationships. J Geotech Geoenviron 2005;131(4):453-464.

[9] Phoon K-K, Kulhawy FH. Characterization of geotechnical variability, Can Geotech J 1999; 36(4):612-624.

[10] Field EH, Jacob KH. Monte-Carlo simulation of the theoretical site response variability at Turkey Flat, California, given the uncertainty in the geotechnically derived input parameters. Earthq Spectra 1993;9(4):669-701.

[11] Idriss IM. Evolution of the state of practice. Int. Workshop on the Uncertainties in Nonlinear Soil Properties and Their Impact on Modeling Dynamic Soil Response. Pacific Earthquake Engineering Research Center, Richmond, California; 2004.

[12] Bazzurro P, Cornell CA. Ground-motion amplification in nonlinear soil sites with uncertain properties. B Seismol Soc Am 2004;94(6):2090-2109.

[13] Bazzurro, P, Cornell CA. Nonlinear soil-site effects in probabilistic seismic-hazard analysis. B Seismol Soc Am 2004; 94(6):2110-2123.

[14] Andrade JE, Borja RI. Quantifying sensitivity of local site response models to statistical variations in soil properties. Acta Geotech 2006; 1(1):3-14.

[15] Sarma SK, Irakleidis A-K. An investigation into the uncertainty of the one dimensional site response analysis. 4th Int Conf Earthq Geotech Eng, Thessaloniki, Greece 25-28 June 2007. Paper No. 1180.

[16] Rota M, Lai CG, Strobbia CL. Stochastic 1D site response analysis at a site in central Italy. Soil Dyn Earthq Eng 2011;31:626-639.

[17] Griffiths SC, Cox BR, Rathje EM, Teague DP. Surface-wave dispersion approach for evaluating statistical models that account for shear-wave velocity uncertainty. J Geotech Geoenviron 2016; 142(11).

[18] Griffiths SC, Cox BR, Rathje EM, Teague DP. (2016b) Mapping dispersion misfit and uncertainty in $_s$ profiles to variability in site response estimates. J Geotech Geoenviron 2016; 142(11).

[19] Teague DP, Cox BR. Site response implications associated with using non-unique V_s profiles from surface wave inversion in comparison with other commonly used methods of accounting for V_s uncertainty. Soil Dynamics and Earthquake Engineering 2016;91:87-103.

[20] Teague DP, Cox BR, Rathje EM. Measured V_s. predicted site response at the Garner Valley Downhole Array considering shear wave velocity uncertainty from borehole and surface wave methods. Soil Dyn Earthq Eng 2018; 113:339-355.

[21] Bahrampouri M, Rodriguez-Marek A, Bommer JJ. Mapping the uncertainty in modulus reduction and damping curves onto the uncertainty of site amplification functions 2019; Soil Dyn Earthq Eng (doi:10.1016/j.soildyn.2018.02.022).

[22] Roblee CJ, Silva WJ, Toro GR, Abrahamson N. Variability in site-specific seismic ground-motion predictions, Uncertainty in the Geologic Environment: From theory to practice. ASCE; 1996.

[23] Li W, Assimaki D. Site-and motion-dependent parametric uncertainty of site-response analyses in earthquake simulations. B Seismol Soc Am 2010;100(3):954-968.

[24] Assimaki D, Li W, Steidl J, Schmedes J. Quantifying nonlinearity susceptibility via site-response modeling uncertainty at three sites in the Los Angeles Basin. B Seismol Soc Am 2008; 98(5):2364-2390.

[25] Rathje EM, Kottke AR, Trent WL. Influence of input motion and site property variabilities on seismic site response analysis. J Geotech Geoenviron 2010; 136(4):607-619.

[26] Toro GR. Probabilistic models of site velocity profiles for generic and site-specific ground-motion amplification studies. Department of Nuclear Energy Brookhaven National Laboratory, Upton, New York; 1995.

[27] Li XS, Shen CK, Wang ZL. Fully coupled inelastic site response analysis for 1986 Lotung earthquake. J Geotech Geoenviron 1998; 124(7):560-573.

[28] Borja RI, Chao HY, Montáns FJ, Lin CH. Nonlinear ground response at Lotung LSST site. J Geotech Geoenviron 1999;125(3):187-197.

[29] Borja, R.I., Chao, H.Y., Montáns, F.J., Lin, C.H. (1999b) SSI effects on ground motion at Lotung LSST site. J of Geotech Geoenviron 1999;125(9):760-770.

[30] Huang H-C, Shieh C-S, Chiu H-C. Linear and nonlinear behaviors of soft soil layers using Lotung downhole array in Taiwan. Terr Atmos Ocean Sci 2001;12(3):503-524.

[31] Borja RI, Duvernay BG, Lin CH. Ground response in Lotung: total stress analyses and parametric studies. J Geotech Geoenviron 2002; 128(1):54-63.

[32] Lee C-P, Tsai Y-B, Wen K-L. Analysis of nonlinear site response using the LSST downhole accelerometer array data. Soil Dynamics and Earthquake Engineering 2016; 26:435-460.

[33] Borja RI, Sun WC. Estimating inelastic sediment deformation from local site response simulations. Acta Geotech 2007; 2:183-195.

[34] Amorosi A, Boldini D, di Lernia A. Seismic ground response at Lotung: Hysteretic elasto-plastic-based 3D analyses. Soil Dyn Earthq Eng 2016; 85:44-61.

[35] Elia G, Rouainia M, Karofyllakis D, Guzel Y. Modelling the non-linear site response at the LSST down-hole accelerometer array in Lotung. Soil Dyn Earthq Eng 2017;102:1-14.

[36] Chan AHC. User Manual for DIANA-SWANDYNE II. University of Birmingham, UK; 1995.

[37] Rouainia M, Muir Wood D. A kinematic hardening constitutive model for natural clays with loss of structure. Gótechnique 2000; 50(2):153-164.

[38] Elia G, Rouainia M. Seismic performance of earth embankment using simple and advanced numerical approaches. J Geotech Geoenviron (2012);139(7):1115-1129.

[39] Elia, G., Rouainia, M. Performance evaluation of a shallow foundation built on structured clays under seismic loading, B Earthq Eng 2014;12(4):1537-1561.

[40] Tang HT, Tang YK, Stepp JC. Lotung large-scale seismic experiment and soil-structure interaction method validation. Nucl Eng Des 1990; 123:197-412.

[41] Anderson DG. Geotechnical synthesis for the Lotung large-scale seismic experiment. Tech. Rep. No. 102362, Electric Power Research Institute, Palo Alto, California; 1993.

[42] Anderson DG, Tang YK. Summary of soil characterization program for the Lotung large-scale seismic experiment. Proc EPRI/NRC/TPC Workshop on Seismic Soil Structure Interaction Analysis Techniques Using Data from Lotung, Taiwan, EPRI NP-6154, Electric Power Research Institute, Palo Alto, California, 1, 4.1-4.20; 1989.

[43] EPRI. Guidance for determining design basis ground motions - Vol.1: Method and guidlines for estimationg earthquake ground motion in Eastern North America. . Rep. No. TR-102293, Electric Power Research Institute , Palo Alto, California.

[44] Viggiani GMB, Atkinson JH. Stiffness of fine-grained soil at very small strains. Géotechnique 1995;45(2):249-265.

[45] Depina I, Le TMH, Eiksund G, Benz T. Behavior of cyclically loaded monopile foundations for offshore wind turbines in heterogeneous sands, Comput and Geotech 2015;65:266-277.

[46] Burland JB. On the compressibility and shear strength of natural clays, Géotechnique 1990; 40(3):329-378.

[47] Rouainia M, Wood DM. Computational aspects in finite strain plasticity analysis of geotechnical materials. Mech Res Commun 2006;33 (2), 123-133

[48] Zhao J, Sheng D, Rouainia M, Sloan SW. Explicit stress integration of complex soil models. Int J Numer Anal Met 2005; 29(12):1209-1229.

[49] Zeghal M, Elgamal AW, Tang HT, Stepp JC. Lotung downhole array. II: Evaluation of soil nonlinear properties. J Geotech Eng 1995; 121(4):363-378.

[50] Elia G, Amorosi A, Chan AHC, Kavvadas M. Fully coupled dynamic analysis of an earth dam. Géotechnique 2011;61(7):549-563.

[51] Chen H, Sun R, Yuan X, Zhang J. Variability of nonlinear dynamic shear modulus and damping ratio of soils. 14th World Conf Earthq Eng, Beijing, China.12-17 October 2008.

[52] Clough RW, Penzien J. Dynamics of Structures. 2nd Edition, McGraw-Hill, New York; 1993.